

NASA TM X- 70858

# GEOS-C ALTIMETER ATTITUDE BIAS ERROR CORRECTION

(NASA-TM-X-70858) GEOS-C ALTIMETER ATTITUDE  
BIAS ERROR CORRECTION (NASA) 16 p HC \$3.25  
CSCL 14B

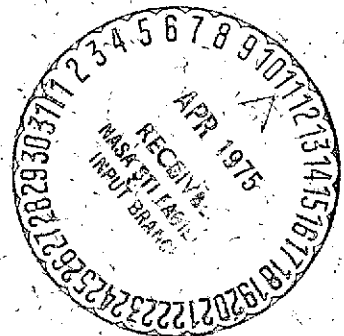
N75-19342

Unclas

G3/19 14169

JOHN W. MARINI

DECEMBER 1974



**GODDARD SPACE FLIGHT CENTER**  
**GREENBELT, MARYLAND**

For information concerning availability  
of this document contact:

Technical Information Division, Code 250  
Goddard Space Flight Center  
Greenbelt, Maryland 20771

(Telephone 301-982-4488)

"This paper presents the views of the author(s), and does not necessarily  
reflect the views of the Goddard Space Flight Center, or NASA."

# **GEOS-C ALTIMETER ATTITUDE BIAS ERROR CORRECTION**

**John W. Marini**

**December 1974**

**Goddard Space Flight Center  
Greenbelt, Maryland 20771**

## CONTENTS

	<u>Page</u>
Introduction . . . . .	1
Expected Return Power . . . . .	1
GEOS-C Altimeter Split Gate Tracking. . . . .	3
Fitting of Error Curves. . . . .	4
Summary . . . . .	6
References . . . . .	6
Appendix APL Programs . . . . .	8

## ILLUSTRATIONS

<u>Figure</u>		<u>Page</u>
1.	Altimeter Geometry. . . . .	8
2.	Altitude Error vs Attitude Error, $\tau = 12.5$ ns . . . . .	9
3.	Altitude Error vs Attitude Error, $\tau = 200$ ns. . . . .	10

PRECEDING PAGE BLANK NOT FILMED

## GEOS-C ALTIMETER ATTITUDE BIAS ERROR CORRECTION

### INTRODUCTION

A pulse-limited split-gate-tracking radar altimeter has been flown on Skylab and will be used aboard GEOS-C [1]. If such an altimeter were to employ a hypothetical isotropic antenna, the altimeter output would, of course, be independent of spacecraft orientation. To reduce power requirements, however, the gain of the altimeter antenna proposed has been increased to the point where its beamwidth is only a few degrees. The gain of the antenna consequently varies somewhat over the pulse-limited illuminated region of the ocean below the altimeter, and the altimeter output varies with antenna orientation. The error thereby introduced into the altimeter data has been modeled empirically [2], but because of an unfortunate choice of the form of the modelling function, close agreements with the expected errors was not realized. In this report the attitude-error effects expected with the GEOS-C altimeter are more closely modelled using a form suggested by an analytical derivation. As in reference [2], the treatment here is restricted to the case of a relatively smooth sea, where the height of the ocean waves are small relative to the spatial length (pulse duration times speed of light) of the transmitted pulse.

### Expected Return Power

The expected value of the received power has been given by Harger [3]. Referring to Figure 1, this power is

$$P_R(t) = \frac{\lambda^2 \sigma_0}{(4\pi)^3 r_0^2} \int_0^{\pi/2} \int_0^{2\pi} \int_{-\infty}^{+\infty} P_T\left(t - \tau_0 - \frac{K r_0 \theta^2}{c} + \frac{2h}{c}\right) G^2(\psi) p(h) \theta dh d\phi d\theta \quad (1)$$

Here

- $P_R(t)$   $\equiv$  Expected value of received power at time  $t$ .  
 $\lambda$   $\equiv$  Wavelength  $\doteq 2.158$  cm for GEOS-C altimeter  
 $\sigma_0$   $\equiv$  Radar cross section of ocean surface per unit area  
 $r_0$   $\equiv$  Satellite height above mean sea level  $\doteq 843$  km for GEOS-C  
 $P_T()$   $\equiv$  Power of transmitted pulse as a function of time  
 $\tau_0$   $\equiv 2r_0/c$  = Roundtrip delay along the vertical\*  
 $K$   $\equiv 1 + r_0/r_e$   $\equiv$  Earth curvature correction  
 $r_e$   $\equiv$  Earth radius  $\doteq 6378$  km  
 $c$   $\equiv$  Speed of light  
 $G(\psi)$   $\equiv$  Antenna gain (assumed symmetric about boresight) as a function of the angle  $\psi$  off boresight  
 $p(h)$   $\equiv$  Probability density function of the departure  $h$  of the sea surface from mean sea level.

In deriving (1) it was assumed that the scattering is spatially incoherent and that the scattering region from which the received power is returned is confined to values of  $\theta$  of less than a few degrees. Over this small angular region  $\sigma_0$  is taken to be constant. With the additional restriction that the sea wave heights are small relative to the pulse length, the first integration in (1) can be performed to give

$$P_R(t) = \frac{\lambda^2 \sigma_0}{(4\pi)^3 r_0^2} \int_0^{\pi/2} \int_0^{2\pi} P_T\left(t - \tau_0 - \frac{Kr_0\theta^2}{c}\right) G^2(\psi) \theta d\phi d\theta \quad (2)$$

There is no loss in generality in taking the line of boresight of the antenna to lie in the  $\phi = 0$  plane at an angle  $\theta_e$  with the vertical. The angle  $\psi$  between boresight and the line  $r$  is then given by

$$\cos \psi = \cos \theta \cos \theta_e + \sin \theta \sin \theta_e \cos \phi \quad (3)$$

---

Neglecting atmospheric effects on propagation, which can be corrected for separately.

Because of the small values assumed for  $\theta$  and  $\theta_e$  this becomes

$$\psi^2 \doteq \theta^2 + \theta_e^2 - 2\theta\theta_e \cos \phi \quad (4)$$

The expected value of the power returned from an incoherently-scattering smooth curved ocean surface may be calculated from equations (2) and (4) if the shape  $P_T$  of the transmitted pulse and the gain function  $G$  of the antenna are known, the calculation being accurate provided that the illuminated area involved in the integration does not extend over more than a few degrees from the vertical.

### GEOS-C Altimeter Split Gate Tracking

The GEOS-C altimeter will employ two gates for tracking [1]. These gates are each one pulse-width wide, and are separated by one pulse-width. The position of the gates is automatically adjusted so that the power in the first is half that in the second. This position then provides a measure of altimeter height, with the time difference between the start of the transmitted pulse and the start of the first gate taken to be the round trip delay time along the vertical. This operation is described by the equation

$$\int_{\tau_m}^{\tau_m + \tau} P_R(t) dt = \frac{1}{2} \int_{\tau_m + 2\tau}^{\tau_m + 3\tau} P_R(t) dt \quad (5)$$

Where  $\tau_m$  is the roundtrip delay time measured by the altimeter and  $\tau$  is the pulse width. If the bias error in this measurement is denoted by  $\tau_e$ , then

$$\tau_m = \tau_0 + \tau_e \quad (6)$$

From (2), (5) and (6)

$$\begin{aligned} & \int_{\tau_e}^{\tau_e + \tau} \int_0^{\pi/2} \int_0^{2\pi} P_T \left( t - \frac{Kr_0 \theta^2}{c} \right) G^2(\psi) \theta d\theta d\phi dt \\ & - \frac{1}{2} \int_{\tau_e + 2\tau}^{\tau_e + 3\tau} \int_0^{\pi/2} \int_0^{2\pi} P_T \left( t - \frac{Kr_0 \theta^2}{c} \right) G^2(\psi) \theta d\phi d\theta dt = 0 \end{aligned} \quad (7)$$

To solve equation (7) above for the bias error  $\tau_e$ , the pulse shape  $P_T$  and the antenna gain function  $G(\psi)$  must be known. Here we assume a rectangular pulse of length  $\tau$

$$\begin{aligned} P_T(x) &= P_0; \quad 0 \leq x \leq \tau \\ &= 0; \quad \text{otherwise} \end{aligned} \tag{8}$$

and, for the antenna, a circular aperture with an illumination that results in

$$G(\psi) = G_0 \frac{\pi^2}{16} \left[ \frac{\sin\left(\alpha + \frac{\pi}{2}\right)}{\alpha + \frac{\pi}{2}} + \frac{\sin\left(\alpha - \frac{\pi}{2}\right)}{\alpha - \frac{\pi}{2}} \right]^2 \tag{9}$$

where

$$\alpha \equiv \frac{\pi a}{\lambda} \sin \psi$$

$$a \equiv \text{diameter of aperture} = 60.96 \text{ cm}$$

Equation (7) was solved for the time delay bias  $\tau_e$  and the corresponding error  $\Delta r_0 = c \tau_e / 2$  in the altimeter height measurement. The left hand side of (7) is a function of  $\tau_e$  whose derivative can be found by means of the usual rule for the differentiation of an integral whose limits depend on a parameter. The solution was consequently readily obtained by numerical integration and the use of the Newton-Raphson method [4]. The APL [5] programs used and a sample calculation using a 200 ns pulse and a 0.1 degree pointing error are given in the Appendix. The bias errors  $\Delta r_0$  for pulse widths of 12.5 and 200 nanoseconds are plotted as solid lines in Figures 2 and 3 respectively.

#### Fitting of Error Curves

In order to use the curves of Figures 2 and 3 in the processing of GEOS-C data, it is desirable to fit the curves with a suitable function. Such a function



could be found by trial and error, but here we have preferred to be guided by an approximate analytic solution to equation (7). First the square of the gain (9), which is an even function of  $\psi$ , was approximated by

$$G^2(\psi) \doteq G_0^2 \left( 1 - A \frac{\psi^2}{\psi_B^2} + B \frac{\psi^4}{\psi_B^4} \right) \quad (10)$$

where

$$\psi_B \doteq \frac{1}{2} \frac{69\lambda}{a} = 1.22^\circ = 0.0213 \text{ radians}$$

is the half beam width. The constants A and B obtained by least squares were about 1.25 and 0.5 respectively. Substituting (10) into (7), the integration may be performed directly. The resulting expression is a quartic equation in  $\tau_e$ . For small values of  $\tau_e$ , ( $\tau_e / \tau \ll 1$ ), the bias error is

$$\Delta r_0 \doteq - \frac{c\tau}{2} \cdot \frac{5}{6} \cdot \frac{\theta_\tau^2}{\psi_B^2} \frac{A - 4B \frac{\theta_e^2}{\psi_B^2} - \frac{12}{5} B \frac{\theta_\tau^2}{\psi_B^2}}{1 - A \frac{\theta_e^2}{\psi_B^2} + B \frac{\theta_e^4}{\psi_B^4} - \frac{5}{3} B \frac{\theta_\tau^4}{\psi_B^4}} \quad (11)$$

where

$$\theta_\tau \doteq \sqrt{\frac{c\tau}{Kr_0}} \text{ radians}$$

An inspection of (11) leads to the conclusion that the altitude error  $\Delta r_0$  is quite sensitive both to the pulse width and, through the dependence on the values of the constants A and B, to the exact shape of the antenna beam. An examination of the magnitude of the terms in (11) suggests the use of the form

$$\Delta r_0 = - a_1 \frac{c\tau}{2} \left( \frac{\theta_\tau}{\psi_B} \right)^2 \left[ 1 - a_2 \left( \frac{\theta_e}{\psi_B} \right)^2 \right] \quad (12)$$

to fit the solid curves of Figures 2 and 3. Using the values  $a_1 = 1.066$  and  $a_2 = 1.348$  obtained by least-squares fitting, the errors given by (12) are plotted as dashed lines on the Figures. Also shown on the Figures are curves calculated from the equation of reference 2.

## Summary

The GEOS-C altimeter bias caused by antenna pointing error has been calculated assuming a calm ocean, a rectangular pulse shape and a specific antenna gain. In the long pulse mode, the bias error is significant, varying over a range of 4 meters as the pointing error varies from 0 to 1.1 degrees. A simple formula is given for correcting this error when the spacecraft attitude is known.

This analysis represents an ongoing NASA-GSFC effort in support of the GEOS-C altimeter capability which has been developed under the direction of the NASA-Wallops Flight Center. Mr. H. Ray Stanley of the Applied Sciences Directorate is the GEOS-C Project Scientist. Mr. C. L. Purdy of the Engineering Directorate, Wallops Flight Center is responsible for GEOS-C altimeter hardware development, data collection, data preprocessing, calibration and data distribution. References 6 and 7 document previous analyses related to the work in this report. This ongoing study is being extended to address sea state effects on satellite altimetry and the results will be published in a subsequent report.

## References

1. GEOS-C Mission, Proposal Briefing Information, Wallops Station, 13 Dec. 1972.
2. T. Godbey, R. Lambert, and G. Milano, "Altitude Errors Arising from Antenna/Satellite Attitude Errors - Recognition and Reduction," NOAA Technical Report ERL 228-AOML 7, Sea Surface Topography from Space, Vol. 1, Feb. 1972.
3. R. Harger, "Radar Altimeter Optimization for Geodesy over the Sea," IEEE Trans Vol. AES-8 No. 6, Nov. 1972.
4. J. Scarborough, "Numerical Mathematical Analysis," The Johns Hopkins Press, Baltimore; 1930.

5. H. Katzan, Jr., "APL Programming and Computer Techniques," Van Nostrand Reinhold Company, N. Y.; 1970.
6. NASA-Wallops Island Station, Technical Plan for Geodetic Earth Orbiting Satellite (GEOS-C) Radar Altimeter System Project, October 1, 1970.
7. L. S. Miller and G. S. Brown, "Engineering Studies Related to the GEOS-C Radar Altimeter," Applied Science Associates under NAS6-2307, May 1974.

## Appendix. APL Programs

```

      VCALT [ ] V
    V CALT T
[1]   THT←(0.3×T÷843000×1+843÷6378)*0.5
[2]   TAU←T
      V
      VN [ ] V
    V Z←FN
[1]   Z←TH×(GAIN PH PST TH)*2
      V
      VGAIN [ ] V
    V Z←GAIN PST;AL
[1]   AL←0(DLA÷LAM)×10PST
[2]   Z←(÷AL)×10AL←AL+1E-8×0=AL←AL+00.5
[3]   Z←Z←Z←+00.25×Z←+(÷AL)×10AL←AL+1E-8×0=AL←AL-01
      V
      VPST [ ] V
    V Z←PH PST TH;ST;STE
[1]   ST←(10TH÷2)*2
[2]   STE←((10THE÷2)+TH×0)*2
[3]   Z←ST+STE-(2×ST×STE)+(0.5×(10TH)×(10THE)×20PH )
[4]   Z←2×-11Z←0.5
      V
      VGA2 [ ] V
    V S←GA2 T;U;V;F;G;D;TH;PH
[1]   U←U,0.5,1-ΦU←0.02544004383 0.1292344072 0.2970774243
[2]   V←V,(256÷1225),ΦV←0.06474248308 0.1398526357 0.1709150253
[3]   D←U×0
[4]   F←THT×(0[T-1])*0.5
[5]   G←THT×(T[0])*0.5
[6]   TH←(F+U×G-F)÷.÷D
[7]   PH←D÷.÷+02×U
[8]   S←02×(G-F)×+/+/ (V÷.÷I)×FN
      V

```

```

      VGA3 [ ] V
    V S+GA3 B;U;W;D;TI;FI;GI;T;TH;PHI;A
[1]  U←U,0.5,1-φU← 0.025446 04383 0.129 2344072 0.2970774243
[2]  V←W,(256÷1225),φV← 0.06 474248308 0.139 85259 57 0.13 09 150253
[3]  D←U×0
[4]  TI←A+U×B-A+0[B-1
[5]  FI←TH×(0[TI-1)*0.5
[6]  GI←TH×TI*0.5
[7]  T←TI°.+.D°.+.D
[8]  TH←((FI°.+.D)+(GI-FI)°.×U)°.+.D
[9]  PHI←D°.+.D°.+.02×U
[10] S←02×(B-A)×+/+/+/+(V°.×W°.×W)×((GI-FI)°.+.D°.+.D)×P N

```

```

      VW GF [ ] V
    V Z←W GF E;NUM
[1]  NUM←(2×GA3 1-E)-GA3 3-E
[2]  Z←E+NUM÷(2×GA2 1-E)+(GA2 2-E)-(GA2 3-E)+2×GA2-E

```

```

      VNR [ ] V
    V Z 1←NR NUM T;N;Z 0
[1]  N←Z 0+0
[2]  STAR T;N←N+1
[3]  Z 1←W GF Z 0
[4]  Z 0←Z 1
[5]  →(N<NUM T)/STAR T
[6]  Z 1←0.5×0.3×TAU×Z 1

```

```

      DIA
6 0.96
      LAM
2.1583
      THE←00.1÷180
      CALT 200
      NR 3
-4.1128

```

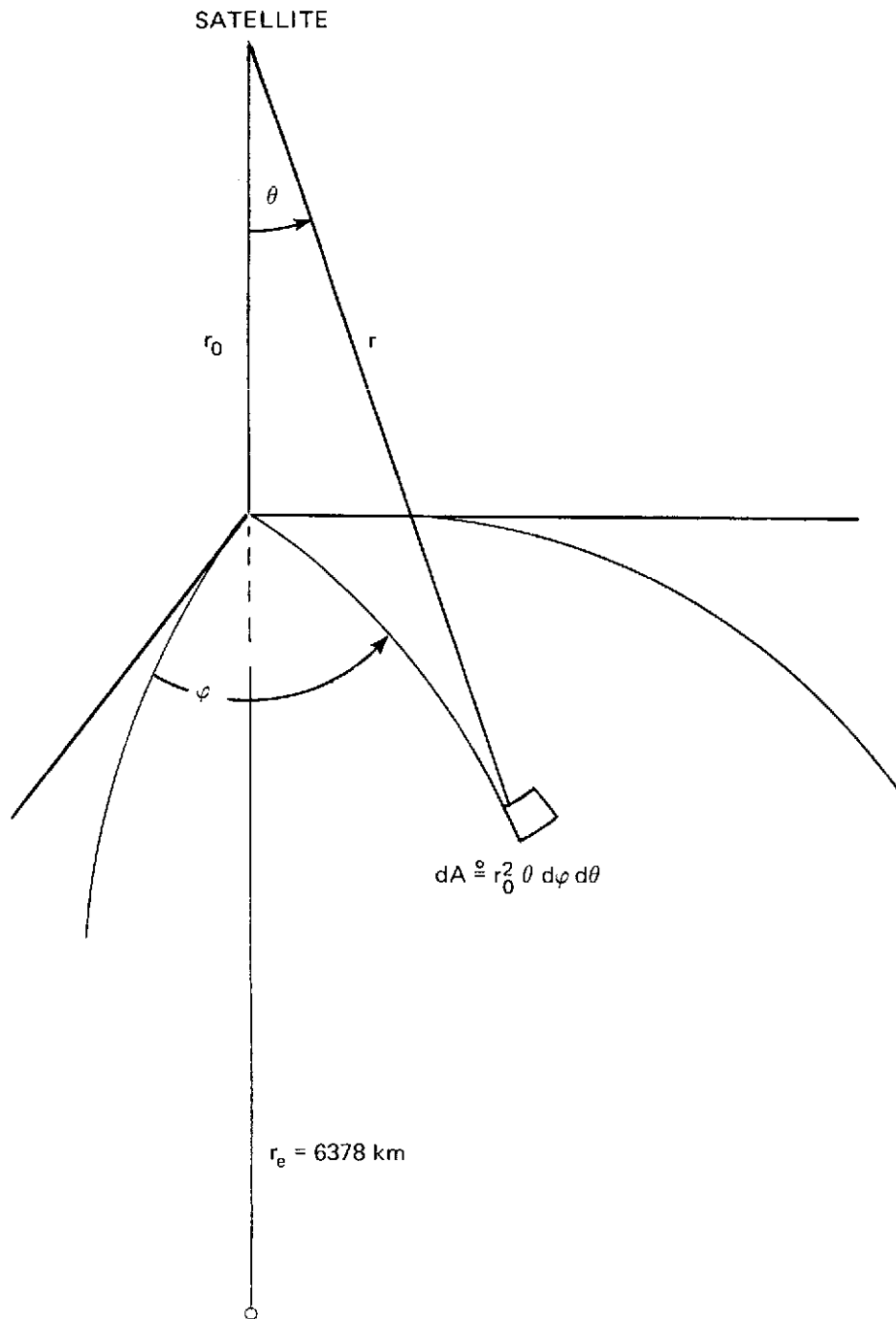


Figure 1. Altimeter Geometry.

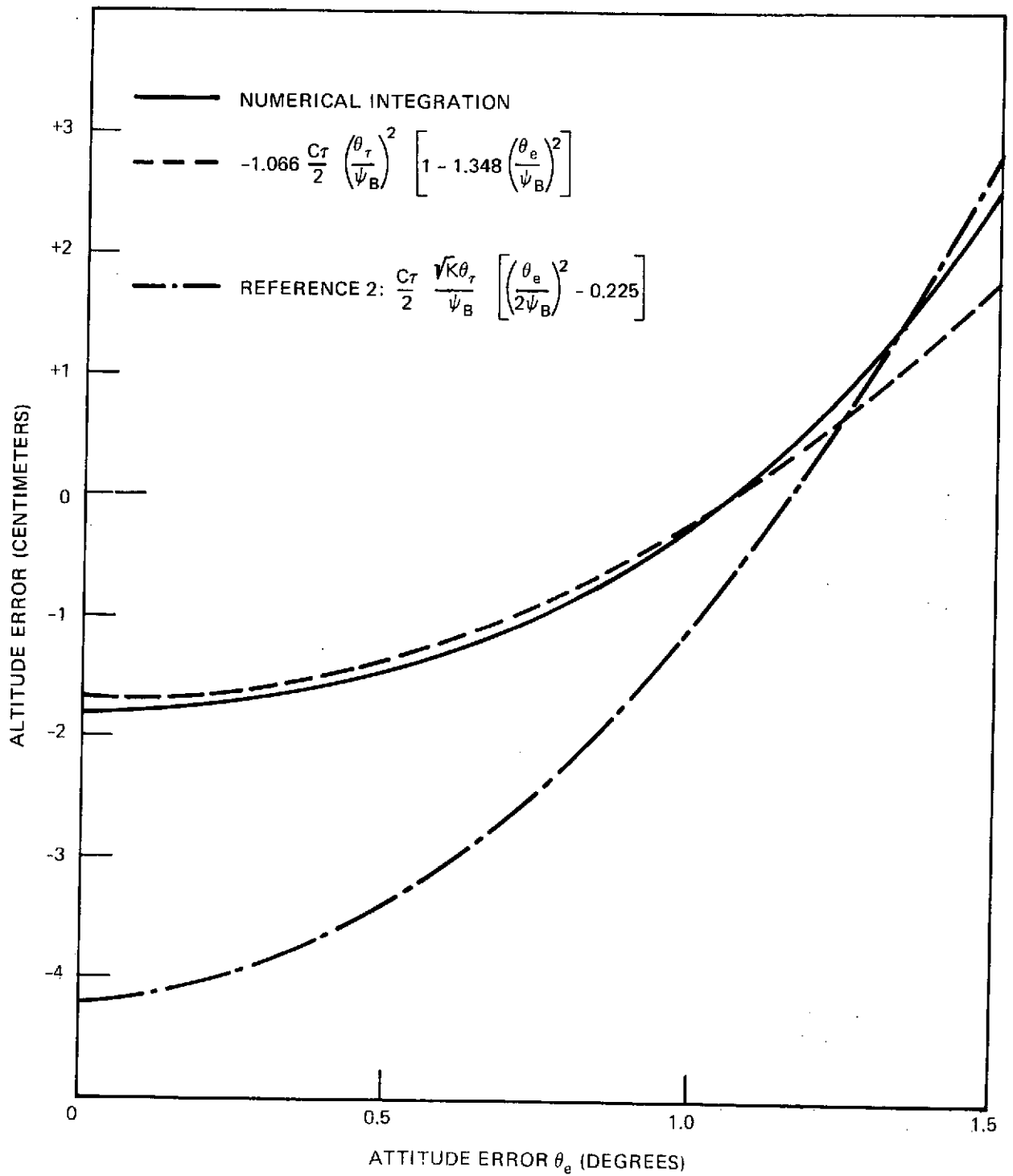


Figure 2. Altitude Error vs. Attitude Error,  $\tau = 12.5$  ns

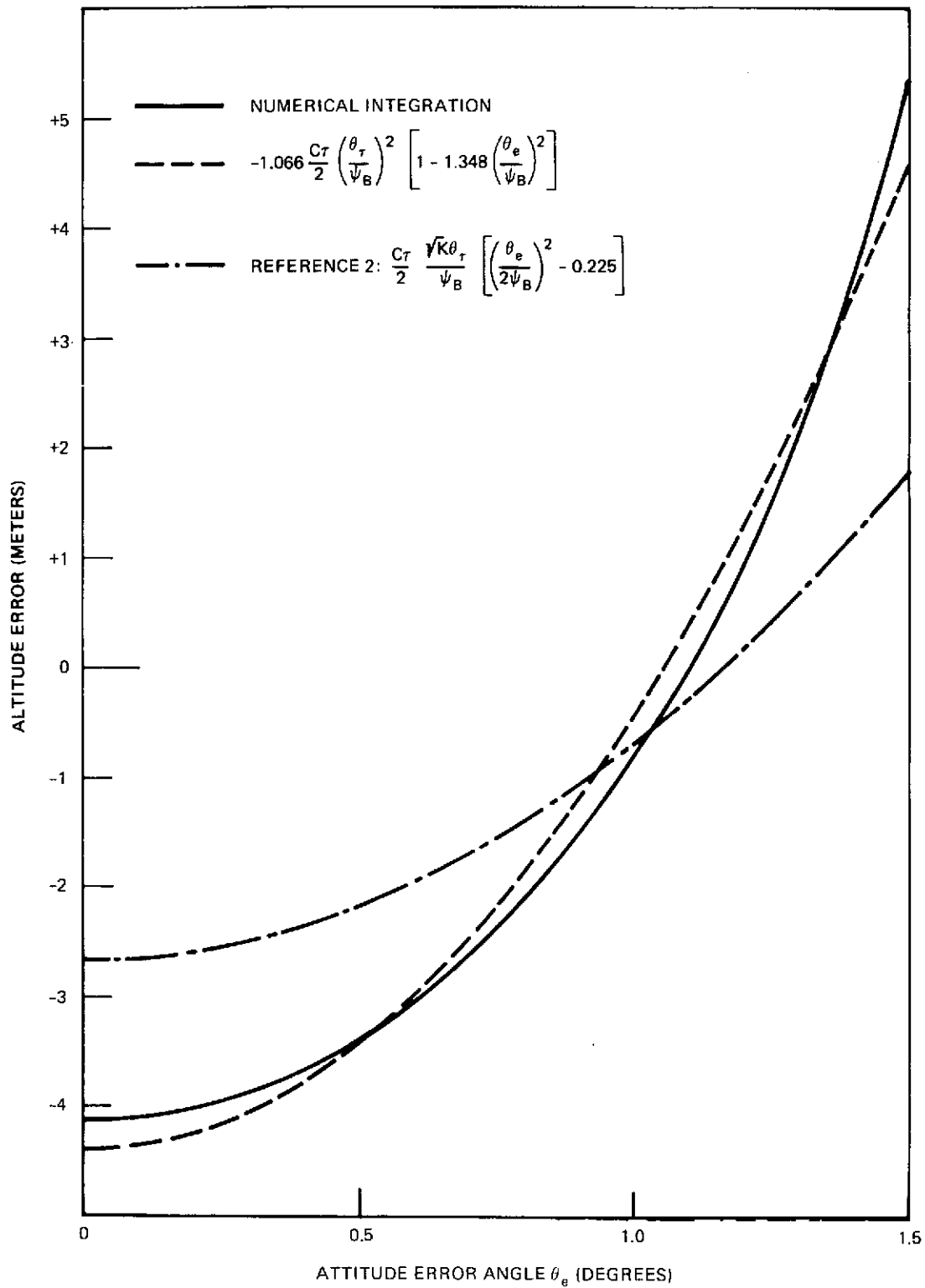


Figure 3. Altitude Error vs. Attitude Error,  $\tau = 200$  ns